

Ultra-high Energy Resolution EELS

Niklas Dellby, Tracy Lovejoy, George Corbin, Nils Johnson, Russel Hayner, Matthew Hoffman, Petr Hrncrik, Benjamin Plotkin-Swing, Dylan Taylor and Ondrej Krivanek

Nion Co., Kirkland, Washington, United States

Vibrational spectroscopy in the electron microscope [1] was recently made possible by combining stable monochromators with ultra-stable electron energy loss (EEL) spectrometers, and continues to progress rapidly. The Nion Iris spectrometer [2] incorporated into the Nion High Energy Resolution Monochromated EELS-STEM (HERMES™) system has led to an EELS era in which < 5 meV energy resolution can be attained at 30 keV primary energy and below. In combination with atom-sized electron probes, introduced just 6 years ago, vibrational spectroscopy has already achieved:

-mapping with isotopic sensitivity, ^{13}C vs ^{12}C in an amino acid (L-alanine) at a specific carbon site, with $\sim 30\text{nm}$ resolution [3]

-probing atomic vibrations at interfaces, and edges of nano-objects, with nm spatial resolution [4]

- 2 \AA -level spatial resolution in the vibrational signal either in the dark-field geometry [5] or in an on-axis geometry in non-polar materials such as silicon [6]

-efficient mapping of acoustic and optical phonons in momentum space with nm spatial resolution using angle-resolved EELS [7]

Figure 1(a) shows a vibrational spectrum from guanine, an essential component of DNA, acquired with 5.9 meV energy resolution at 30 kV. This vibrational fingerprint is quite rich in structure--there are >10 distinct peaks below 200meV. While 5-6 meV resolution already allows for many interesting applications, it is clear that better resolution will yield still richer structure for many materials.

The HERMES system has recently attained 2.98 meV FWHM (full width at half-maximum) of the zero loss peak (ZLP) at 20kV shown in figure 1 (b). This presentation will describe our ongoing efforts to improve the capabilities of EEL spectroscopy via:

1. Optimizing the size of the slit-level crossover. The ultimate energy resolution at the sample is given by the ratio of the size of the slit-level crossover to the energy dispersion at the slit. In exact analogy with the sample-level crossover (i.e. the demagnified image of the electron source, also known as “the probe”), the slit-level crossover size is determined by the diffraction-limited size of the source image given by the incident angles (chosen so that aberrations do not affect the probe formation), and broadened by finite source size. Using the slit to select 3meV out of the intrinsic 300meV CFE energy width reduces the current by 100x or more, which exacerbates the familiar compromise between beam current and probe size by roughly two orders of magnitude.

Similar to probe formation, the effect of finite source size at the slit can be reduced by increasing the angles - i.e. by correcting the aberrations of the image of the source at the slit, and increasing the range of admitted angles correspondingly. The Nion monochromator includes sextupoles and octupoles in a mini C3 corrector before the slit, and it is straightforward to correct 2nd and 3rd order aberrations at the slit using autotuning.

2. Minimizing the instabilities in the total system. This is accomplished using: a ground-potential monochromator system design including stabilization schemes that remove the sensitivity to strongest elements in the system (the high voltage and the primary prism supply), application of the same rigorous stability and shielding design standards as those used in the pre-sample column all the way from the sample to the final detector, ultra-stable power supplies, and a stable microscope environment.

3. Improving the tails of the ZLP. As shown in Figure 1(a), while the ZLP FWHM is a key factor, practical work relies on the ZLP tails at the $1/10^4$ level and below. There are two principal contributions to the tails. First, the energy distribution coming out of the monochromator, which is determined by a convolution of the crossover at the monochromator slit and the slit itself. And second, spreading in the post sample column/detection system due to scattering from residual gasses and beam spreading in the final detector. These are addressed using ultra-high-vacuum, low-spread detectors, and ultra-high energy dispersion at the detector, such as ~ 0.1 meV/channel.

Further practical gains come from increasingly user-friendly operation/processing, flexible operation modes, and better detectors. For example, a new generation of direct detector for EELS with 10^7 dynamic range and no readout noise greatly benefits ultra-high resolution EELS [7].

As the EELS energy resolution improves beyond 5 meV, the requirements on the system increase substantially. Optimization in the key areas described above will lead further into the era of diffraction-limited EELS in which < 5 meV and ultimately 1-2 meV become routine. The benefits for vibrational spectroscopy promise to be immense.

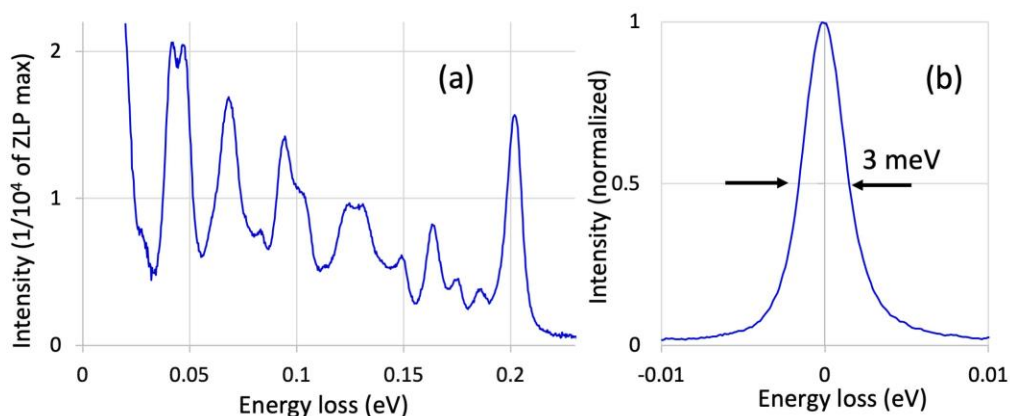


Figure 1. (a) Vibrational spectra of guanine acquired with 5.9 meV resolution at 30kV (vacuum ZLP is subtracted, 100 ms x 2,000, 1 pA), and (b) ZLP with 2.98 meV FWHM acquired at 20kV (333 x 3ms, $a/2=b/2=15$ mrad, 0.125 meV/ch.).

References

- [1] O.L. Krivanek et al., *Nature* **514** (2014) 209; T. Miata et al., *Microscopy* **63** (2014) 377
- [2] T.C. Lovejoy et al., *Microsc. Microanal.* **24** (Suppl 1, 2018) 446-447
- [3] J. Hachtel et al., *Science* **363** (2019) 525–528
- [4] MJ Lagos and PE Batson, *Nature*, **543**, 529-532(2017), C. Dwyer et al., *Phys. Rev. Lett* **117** (2016) 256101
- [5] F.S. Hage et al., *Phys. Rev. Lett* **122** (2019) 016103
- [6] K. Venkatraman et al., *Nat. Phys.* **15**, 1237-1241(2019)
- [7] T.C. Lovejoy et al., *Microsc. Microanal.* **25** (Suppl 2, 2019) 628-629, *and these proceedings*